Supplement of Atmos. Chem. Phys., 18, 2601–2614, 2018
https://doi.org/10.5194/acp-18-2601-2018-supplement

Atmospheric Chemistry and Physics
Open Access
EGU

Supplement of

Effects of temperature-dependent NO_x emissions on continental ozone production

Paul S. Romer et al.

Correspondence to: Ronald C. Cohen (rccohen@berkeley.edu)

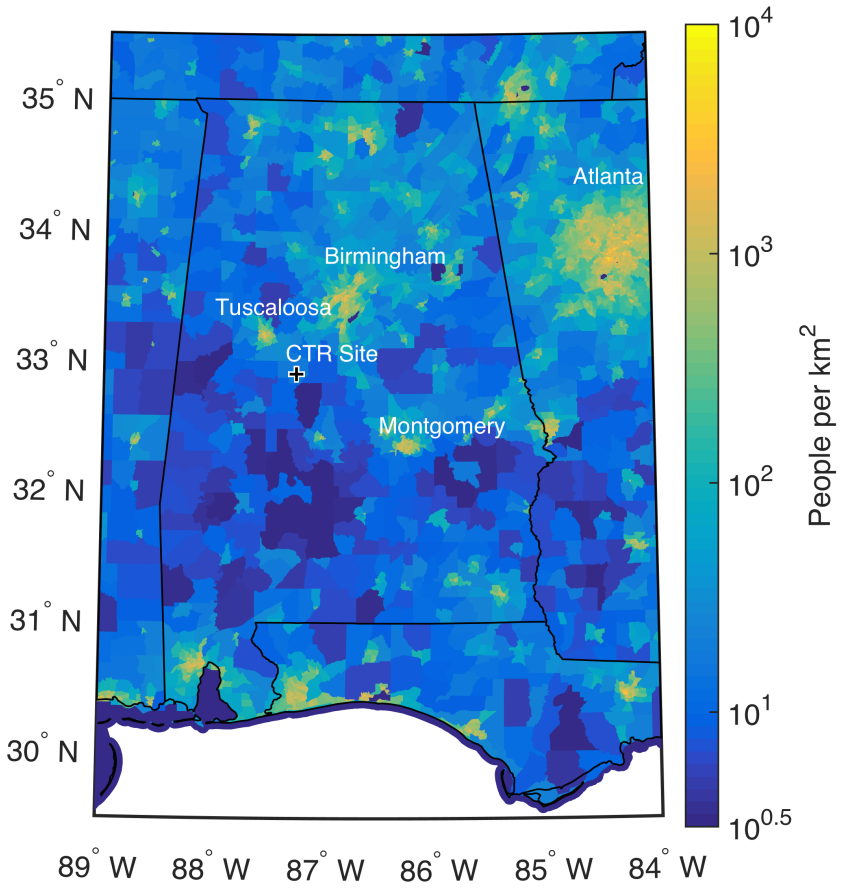

Figure S1: Map of Alabama showing the CTR site (black cross) and major population centers. Population density is from the 2010 US Census.

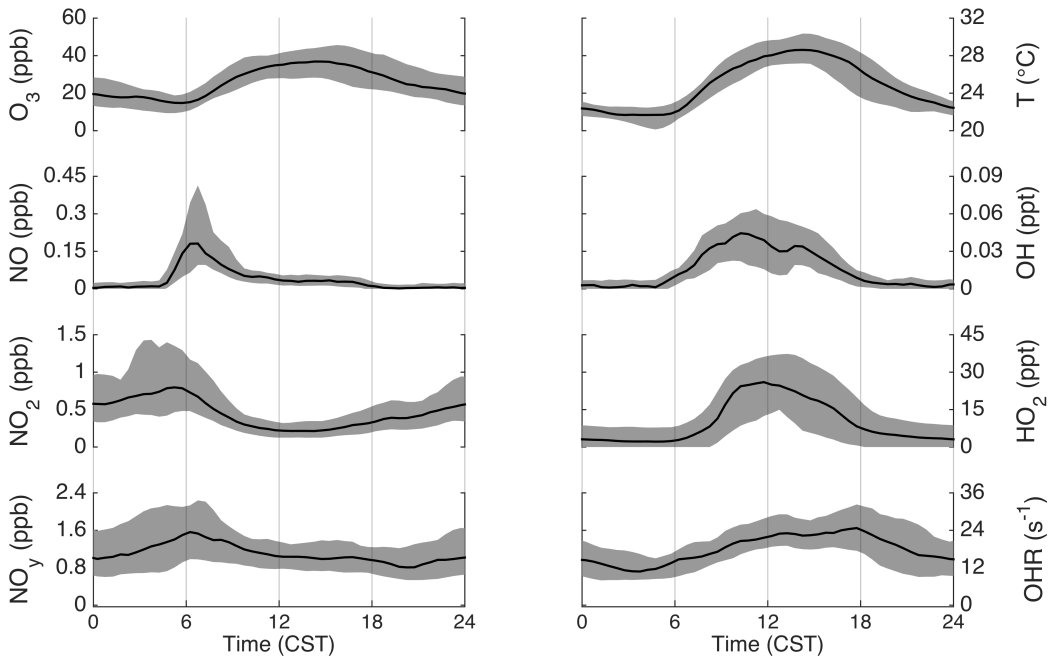

Figure S2: Diurnal cycle of the primary parameters used in this study as measured during SOAS. For each quantity the black line shows the hourly median and the shaded gray area shows the interquartile range.

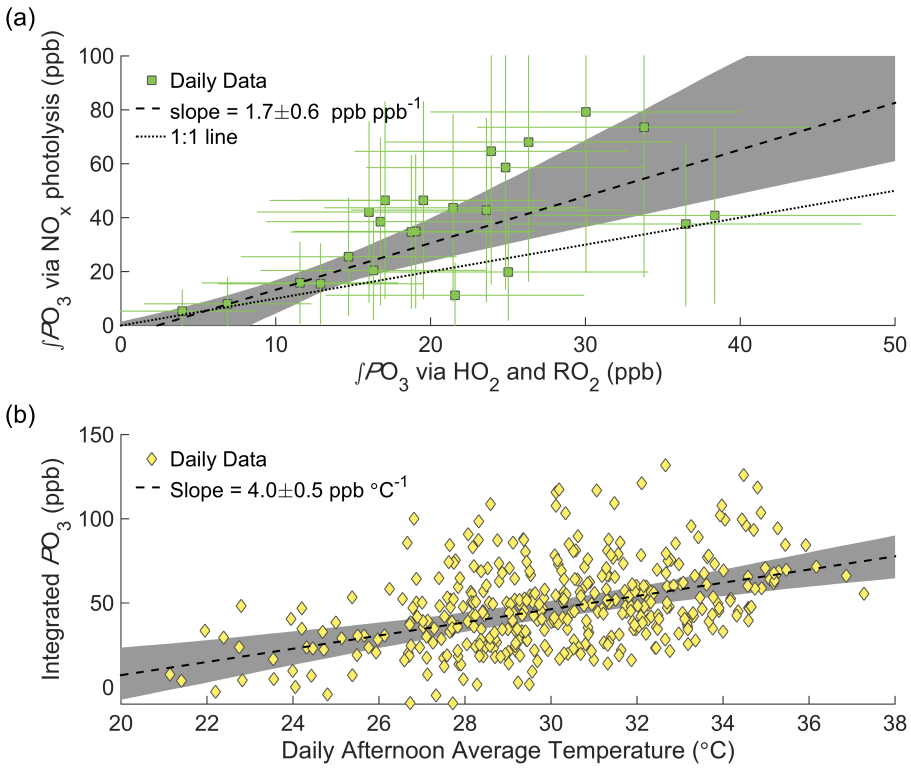

Figure S3: Comparison of daily integrated ozone production via two methods (a) and long-term trend in $\int PO_3$ with temperature (b). The reported slope in panel (a) was calculated using a bivariate (York-type) fit accounting for the error in both x and y.

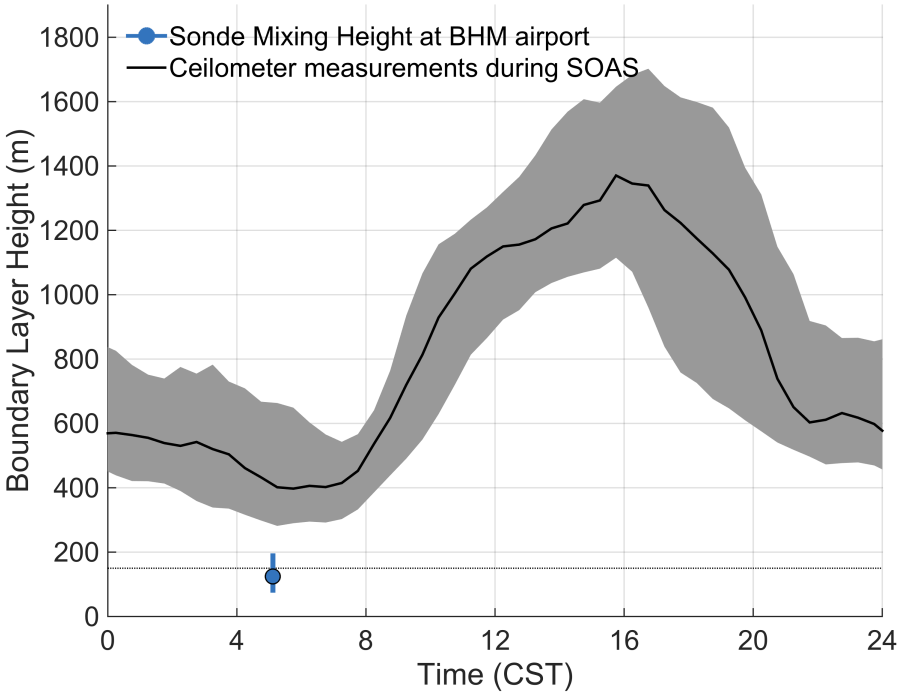

Figure S4: Measurements of the boundary layer height during SOAS as measured by ceilometer (black line) and the inversion height at the BHM airport as measured by radiosonde (blue circle and bar).

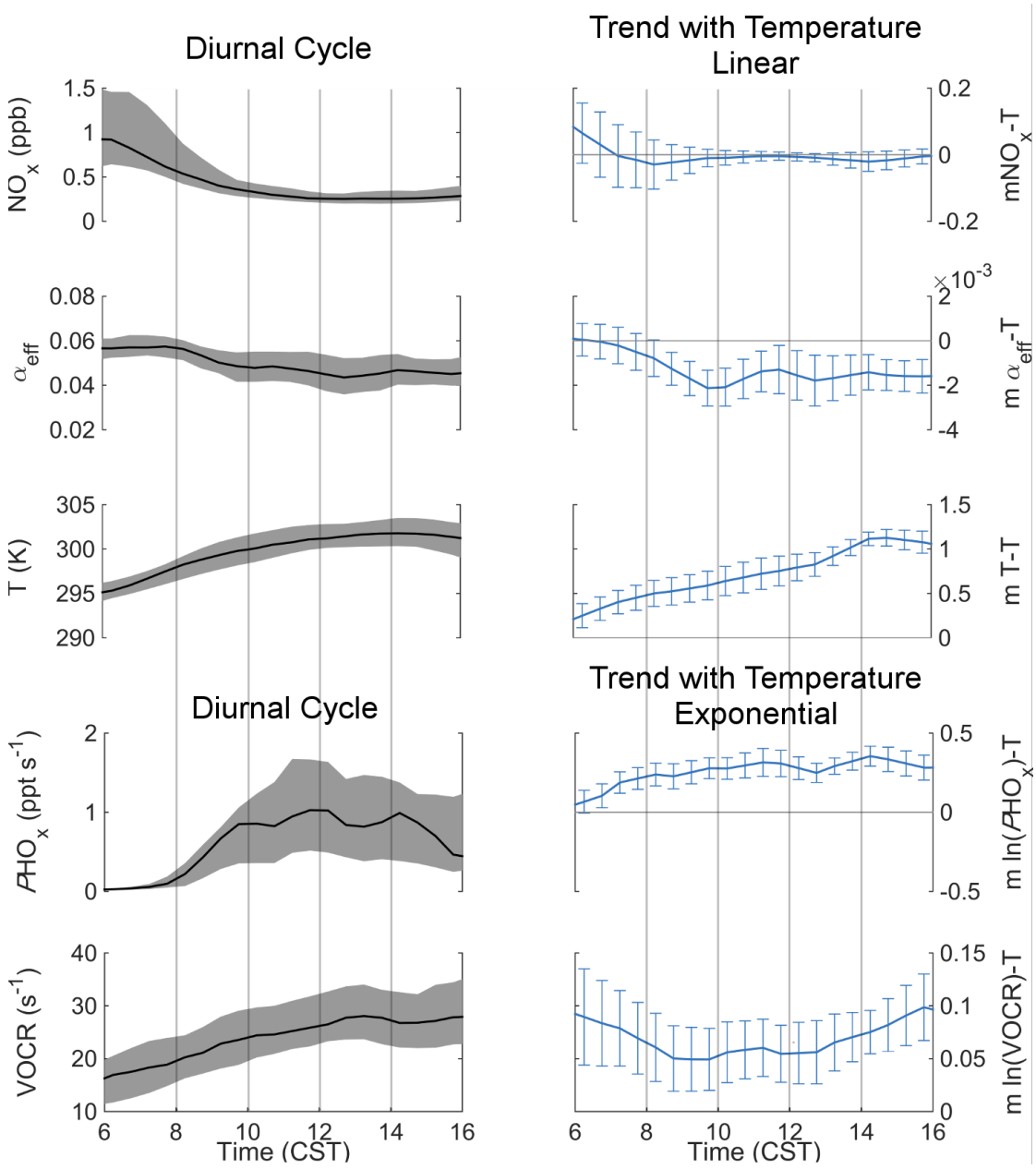

Figure S5: Measurement inputs for the O_3-T decomposition, showing the observed diurnal cycle (left side) and trend with temperature (right side). The trends for VOCR and $P\mathrm{HO_x}$ are reported on a log-scale, representing an expected exponential increase with temperature. In the left column, the black lines and shaded gray areas show the median and interquartile range for each parameter; in the right column the line and error bars show the calculated trend and its associated uncertainty from a least-squares regression.

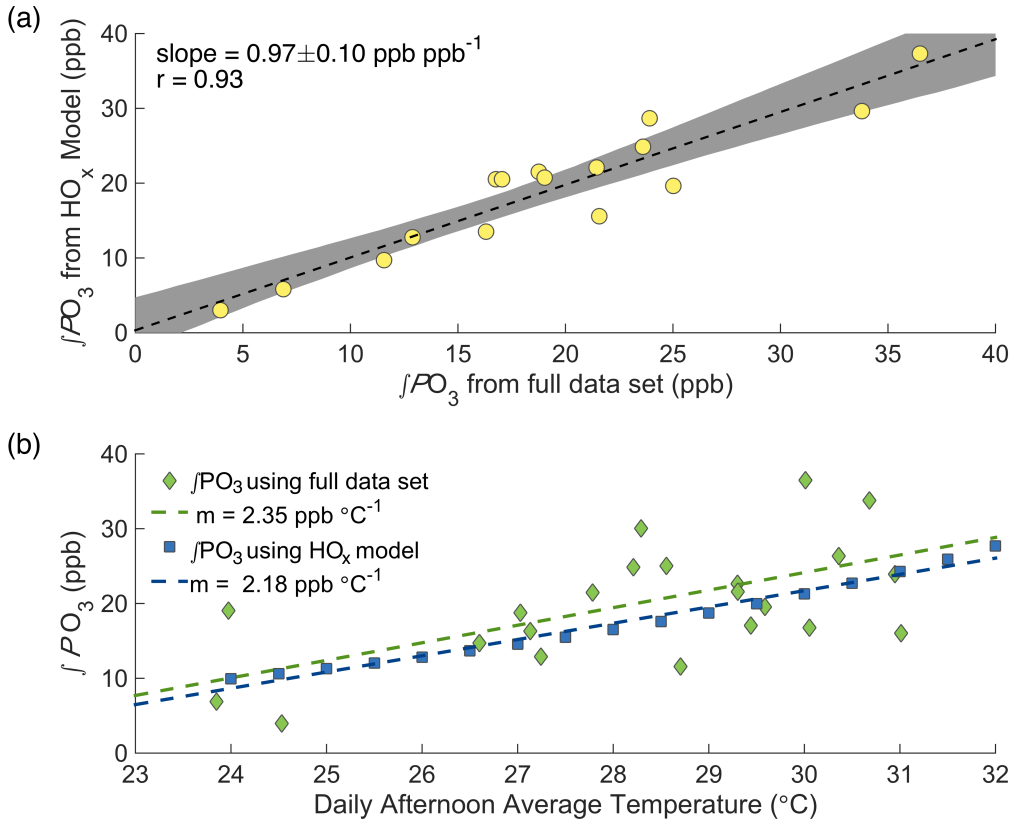

Figure S6: Panel (a): Comparison of $\int PO_3$ based on the full data set and simplified HO_x model; Panel (b): comparison of the $\int PO_3$-T trend using all data (green diamonds) and HO_x model using only the diurnal cycle and trend with temperature of the inputs (blue squares).

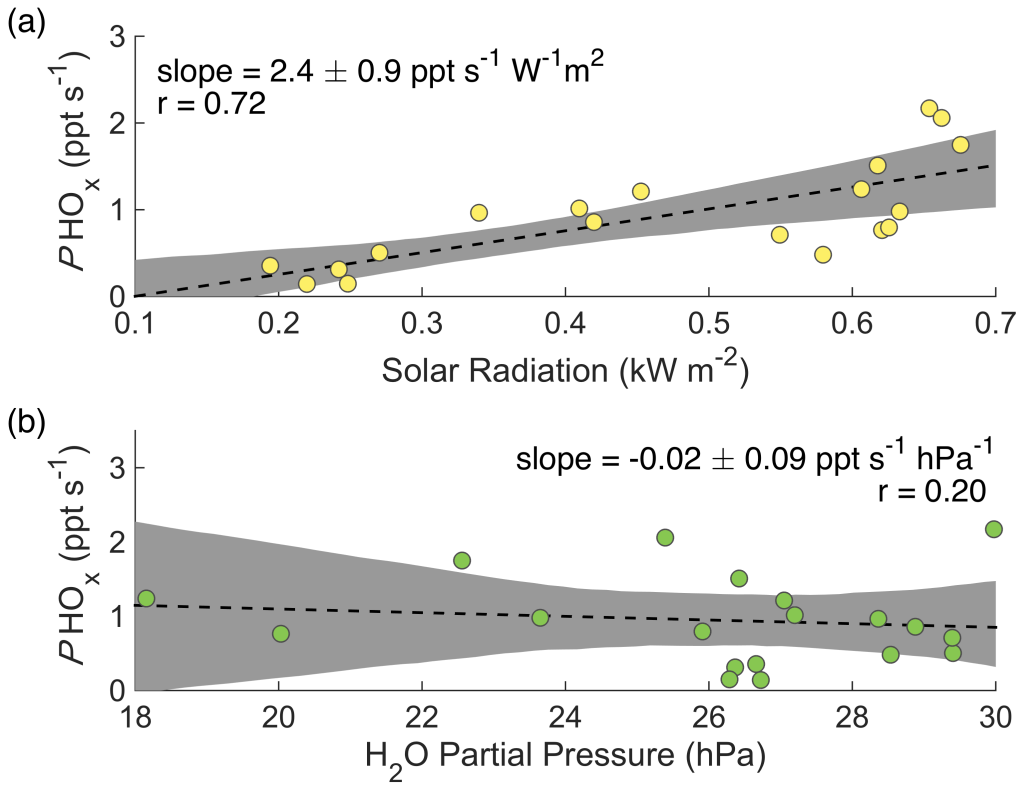

Figure S7: Correlation of total daily average afternoon $P\mathrm{HO_x}$ with daily average afternoon solar radiation (a) and daily average afternoon water vapor concentration (b).

Table S1: VOC Inputs for calculating RO_2 concentrations. Unless otherwise noted compounds were measured by GC-MS and values of α_i were obtained from *Perring et al.* (2013).

Compound	α_i	k_{OH}[a]	Avg. Conc.[a]	Avg. Reactivity[a]
		cm^3 $molec^{-1}$ s^{-1}	ppt	s^{-1}
Isoprene	0.12[b]	9.91e-11	4.6e+03	1.1e+01
CO[e]	0	2.27e-13	1.3e+05	7.3e-01
MVK[f]	0.035	1.99e-11	9.1e+02	4.3e-01
Acetaldehyde	0	1.48e-11	1.1e+03	4.0e-01
β-Pinene	0.23	7.82e-11	2.0e+02	3.9e-01
MACR[f]	0.014[c]	2.84e-11	4.4e+02	3.0e-01
Methane[g]	0.001	6.62e-19	1.7e+06	2.9e-01
α-Pinene	0.26[d]	5.20e-11	2.3e+02	2.9e-01
Limonene	0.23	1.63e-10	6.8e+01	2.7e-01
Methanol	0	9.02e-13	7.7e+03	1.7e-01
Ethanol	0.01	3.21e-12	1.9e+03	1.5e-01
Ethene	0.01	7.78e-12	3.3e+02	6.2e-02
Propanal	0	1.97e-11	8.6e+01	4.1e-02
Propene	0.01	2.84e-11	5.1e+01	3.5e-02
Propane	0.04	1.08e-12	8.3e+02	2.2e-02
Butanal	0	2.35e-11	3.1e+01	1.7e-02
2-Ethyltoluene	0.03	1.87e-11	2.4e+01	1.1e-02
iPentane	0.07	3.60e-12	1.2e+02	1.0e-02
Ethane	0.02	2.46e-13	1.5e+03	9.0e-03
nButane	0.08	2.38e-12	1.6e+02	9.0e-03
Acetone	0	1.78e-13	2.0e+03	8.8e-03
mXylene + pXylene	0.03	1.80e-11	2.0e+01	8.7e-03
1,3,5-Trimethylbenzene	0.03	5.67e-11	5.9e+00	8.2e-03
nPentane	0.10	3.84e-12	8.7e+01	8.1e-03
Toluene	0.03	5.59e-12	5.4e+01	7.4e-03
Butanone	0	1.11e-12	2.7e+02	7.3e-03
1,2,4-Trimethylbenzene	0.03	3.25e-11	7.8e+00	6.2e-03
iButane	0.10	2.09e-12	8.4e+01	4.3e-03
nDecane	0.42	1.10e-11	1.2e+01	3.2e-03
oXylene	0.03	1.22e-11	9.2e+00	2.7e-03
Ethylbenzene	0.03	7.00e-12	9.6e+00	1.6e-03
Benzene	0.03	1.22e-12	5.4e+01	1.6e-03

[a] 6 am–4 pm Average
[b] Value from *Teng et al.* (2017)
[c] RO_2 isomers that undergo rapid isomerization are not included
[d] Value from *Rindelaub et al.* (2015)
[e] Measured by ARA
[f] Sum measured by PTR-TOF-MS
[g] Not measured during SOAS, a constant value of 1750 ppb assumed

Table S2: Observed trend in NO_y with temperature at 6 SEARCH sites across all days June–August 2010–2014. GFP data only extends through 2012.

Site Name	Location	mNO_y-T (ppb $°C^{-1}$)
CTR	Rural	0.072 ± 0.009
YRK	Rural	0.043 ± 0.015
OAK	Suburban	-0.034 ± 0.016
JST	Urban	-0.037 ± 0.047
BHM	Urban	-0.312 ± 0.050
GFP	Urban	-0.050 ± 0.040

Supplementary References

Perring, A. E., S. E. Pusede, and R. C. Cohen, An Observational Perspective on the Atmospheric Impacts of Alkyl and Multifunctional Nitrates on Ozone and Secondary Organic Aerosol, *Chem. Rev.*, *113*, 5848–5870, doi: 10.1021/cr300520x, 2013.

Rindelaub, J. D., K. M. McAvey, and P. B. Shepson, The photochemical production of organic nitrates from α-pinene and loss via acid-dependent particle phase hydrolysis, *Atmos. Environ.*, *100*, 193–201, doi: 10.1016/j.atmosenv.2014.11.010, 2015.

Teng, A. P., J. D. Crounse, and P. O. Wennberg, Isoprene Peroxy Radical Dynamics, *J. Am. Chem. Soc.*, *139*(15), 5367–5377, doi: 10.1021/jacs.6b12838, 2017.